10.24425/acs.2023.148879

Archives of Control Sciences
Volume 33(LXIX), 2023
No. 4*, pages 737–759*

Navigation and mapping of closed spaces with a mobile robot and RFID grid

Bartosz PAWŁOWICZ, Mariusz SKOCZYLAS, Bartosz TRYBUS, Mateusz SALACH, Marcin HUBACZ and Damian MAZUR

This article concerns the use of an integrated RFID system with a mobile robot for the navigation and mapping of closed spaces. The architecture of a prototype mobile robot equipped with a set of RFID readers that performs the mapping functions is described. Laboratory tests of the robot have been carried out using a test stand equipped with a grid of appropriately programmed RFID transponders. A simulation model of the effectiveness of transponder reading by the robot has been prepared. The conclusions from measurements and tests are discussed, and methods for improving the solution are proposed.

Key words: mobile robot, space mapping, RFID

1. Introduction

The use of RFID technology in the indoor mapping and navigation of autonomous robots is the subject of many scientific studies [1–3]. The size of the information contained in passive or semi-passive identifiers significantly exceeds the commonly used barcodes [4]. The proposed systems can be used in many

B. Pawłowicz (e-mail: barpaw@prz.edu.pl) and M. Skoczylas (e-mail: msko@prz.edu.pl) are with Department of Electronic and Telecommunications Systems, Rzeszów University of Technology, Wincentego Pola 2, 35-959 Rzeszow, Poland.

B. Trybus and M. Hubacz (e-mail: m.hubacz@prz.edu.pl) are with Department of Computer and Control Engineering, Rzeszow University of Technology, Wincentego Pola 2, 35-959 Rzeszow, Poland.

M. Salach (e-mail: m.salach@prz.edu.pl) is with Department of Complex Systems, Rzeszow University of Technology, Wincentego Pola 2, 35-959 Rzeszow, Poland.

D. Mazur (corresponding author, e-mail: mazur@prz.edu.pl) is with Department of Electrical and Computer Engineering Fundamentals, Rzeszow University of Technology, Wincentego Pola 2, 35-959 Rzeszow, Poland.

This project is financed by the Minister of Education and Science of the Republic of Poland within the “Regional Initiative of Excellence” program for years 2019–2022. Project number 027/RID/2018/19, amount granted 11 999 900 PLN.
The authors declare no conflict of interest.

Received 28.12.2022. Revised 11.11.2023.

areas of the ISM area (industrial, scientific, medical). Building surface exploration and mapping with such robots is also a promising area of research [5, 6]. The development of autonomous mobile robots used in logistics, manufacturing, mining, warehouses, and buildings makes it possible to actively use direction data provided by the environment. In the field of navigation, RFID is usually an alternative solution to the systems based on signals from the Global Positioning System (GPS) in conditions where the GPS signal is unavailable, e.g., indoors, warehouses, factories, tunnels, etc.

Contemporary experimental RFID navigation systems assume equipping mobile robots with the Read/Write Device (RWD, later called the RFID reader) that enable them to get data from transponders located in the space where the robot navigates. An attempt can be made to determine the position and direction of an object equipped with the RFID reader by analyzing data from transponders placed in known space locations [7–9]. Many of the existing studies are based on the use of the RSSI (Received signal strength indicator) method [10–12]. To increase the accuracy of position estimation, additional procedures such as odometry or Extended Kalman filter can be used [13]. Original solutions have also been developed, based on measurements of the phase of the signal reflected from the transponder and the transfer of the read information [14].

However, the above-mentioned research is based on highly developed mathematical methods, while omitting the possibility of supporting the location using data stored in the memory of each transponder. This gap was noticed very quickly, which resulted in the development of various methods to determine the position and orientation of an object equipped with the RFID reader. The approaches range from basic ones providing guidelines on data reading [15] to sophisticated solutions employing the measurement of signal strength reflected from transponders in the environment [16, 17]. The solutions range from simple ones that inform how the data should be read to advanced solutions using the measurement of the strength of signals reflected from transponders in space.

RFID transponders are placed at designated points that make up a grid to provide the robot with information about the current coordinates and the environment in which the robot is moving (Fig. 1). As a result, the robots move according to the predetermined trajectory (navigation) and gain knowledge about the configuration of the interior in which they move. Thus, it is possible to map the interior by the robot, as well as record and locate the surrounding interior equipment [18–20]. RFID transponders placed on the floor, walls, and objects can encode information and coordinates used to navigate the robot [21]. In general, transponders are assumed to carry static information, that is, they are preprogrammed with readonly data, while the mobile robot is responsible for processing the information and creating a room map of the room on its basis [22, 23].

The transponders located at the grid nodes are equipped with a single antenna, which enables them to be powered and respond to the queries of the reader in-

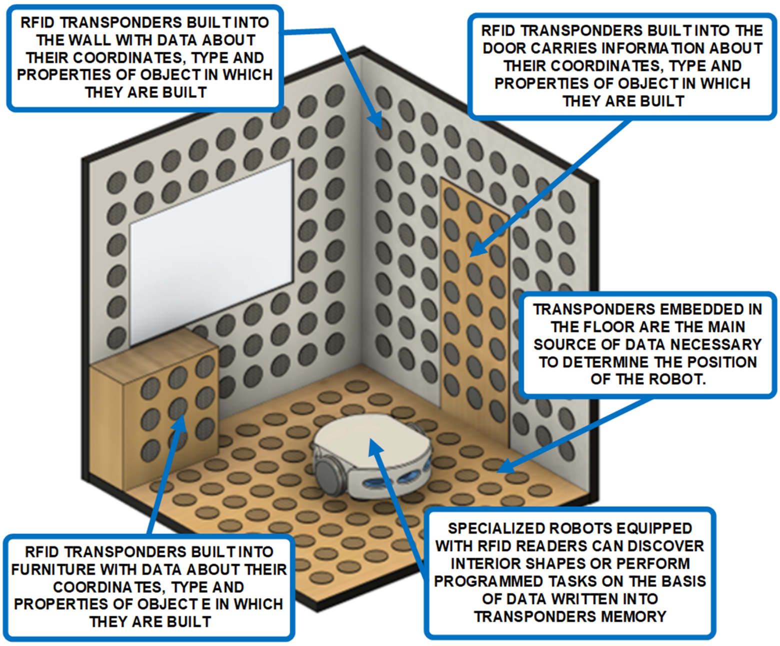

Figure 1: An example of the use of RFID grid in closed spaces

stalled in the robot. Transponders generally have two areas of memory: readable memory and writable memory [24]. The read-only memory stores the serial number of the transponder, information about the coordinates in which the transponder is located, and the type of object on which it is placed (e.g., door, wall, floor). The writable memory, on the other hand, can be used to record information about objects that dynamically appear in the environment or change their location.

However, it is important that the most common solutions use one reader in a mobile robot. Robots with a single centrally located reader are characterized by a limited measurement accuracy, which imposed huge limitations [25]. To improve the estimated position of the robot, it was decided to equip the system with multiple readers, which results in correcting the accuracy of the position approximation.

2. Operation of the RFID system

An important aspect of the operation of devices that use radio communication is to ensure uninterrupted operation of the RFID readers. This is required for proper power and data exchange with transponders located in space [26–28]. The efficiency of the RFID system can be fully expressed by the parameter called the interrogation zone [29, 30]. This area describes the energy and communication conditions of RFID system [26, 31]. Energy in RFID systems is carried by an electromagnetic field, so each of these systems must comply with acceptable radiation standards based on the CEPT/ERC 70-03 recommendations. Based on these guidelines, it is possible to determine the minimum field strength needed to power transponders [32, 33].

In RFID systems, two types of solutions that define energy transmission can be distinguished that define energy transmission. The first is inductive coupling systems and the second is propagation coupling [30, 34]. The low- and high-frequency bands are used in the first [26]. The energy transferred between the reader and the transponder is sent by the magnetic field (Fig. 2), and its amount depends on the area and relative position of the antennas [32]. For proper function, it is necessary to activate the RFID transponder antenna at the resonant frequency, as it causes maximum current to flow in the antenna circuit [30, 34, 35].

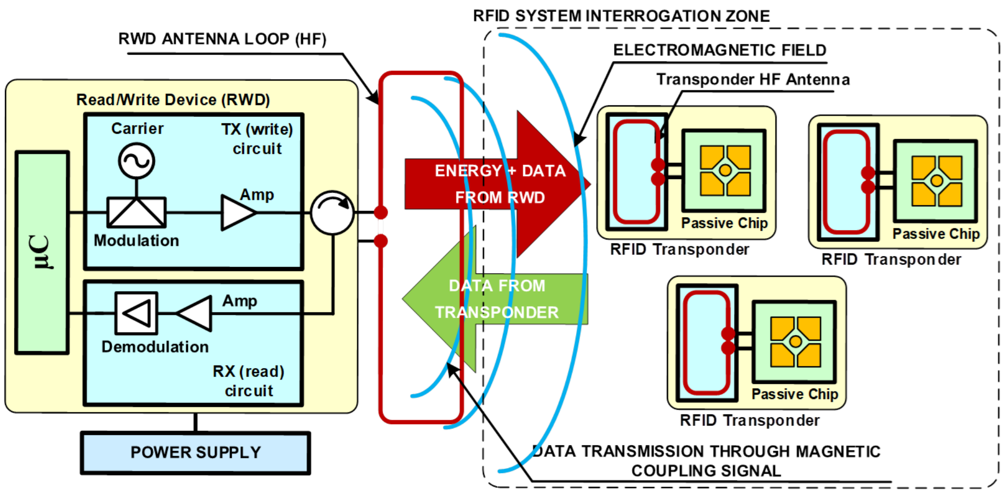

Figure 2: General diagram of the inductive coupled RFID identification system

RFID technology uses inductive coupling. Usually passive transponders are used most often. Here, each transponder located in the polling zone sends its data continuously [37, 38]. In the case of inductive coupling, the maximum range is possible when the transponder antenna coil is perpendicular to the magnetic field lines generated by the reader antenna. On the other hand, in a parallel arrangement, it is not possible to supply energy to the identifier. In addition, the achievable range of readers is strongly dependent on administrative restrictions on the maximum magnetic field strength generated by the reader antenna [39].

Acceptable limits vary between countries and are included in the ETSI standards. The exchange of information between the passive transponder and the RFID reader is modulated by the carrier's reflection coefficient (backscatter) [40, 41].

This is achieved by changing the load on the transponder antenna [32]. The effect is a partial reflection of the wave energy that reaches the transponder in the opposite direction. When the change in the intensity of this field is read, it is possible to demodulate the signal and obtain the information sent. Correct data transmission between the elements of the above-mentioned system involves the use of appropriate modulation, so the energy transmitted to the transponder belts will be sufficient [30, 32, 33, 44, 45]

RFID technology uses inductive coupling. Usually passive transponders are used most often. Here, each transponder located in the polling zone sends its data continuously [37, 38]. In the case of inductive coupling, the maximum range is possible when the transponder antenna coil is perpendicular to the magnetic field lines generated by the reader antenna. On the other hand, in a parallel arrangement, it is not possible to supply energy to the identifier. In addition, the achievable range of readers is strongly dependent on administrative restrictions on the maximum magnetic field strength generated by the reader antenna [39]. Acceptable limits vary between countries and are included in the ETSI standards.

The exchange of information between the passive transponder and the RFID reader is modulated by the carrier's reflection coefficient (backscatter) [40, 41]. This is achieved by changing the load on the transponder antenna [32]. The effect is a partial reflection of the wave energy that reaches the transponder in the opposite direction. When the change in the intensity of this field is read, it is possible to demodulate the signal and obtain the information sent. Correct data transmission between the elements of the above-mentioned system involves the use of appropriate modulation, so the energy transmitted to the transponder belts will be sufficient [30, 32, 33, 44, 45].

3. Autonomous mobile robot

As part of the research, a robot mapping a closed surface was developed and built with the use of RFID technology. The constructed robot is a mobile platform moving inside the enclosure, which is a closed, limited space. To simplify the complexity of the control and control algorithms, it was assumed that the space is static, i.e. it does not change during a single mapping run.

The supporting structure of the robot is made entirely of plastic that does not interfere with the operation of RFID readers. The STM32F303RE microcontroller with the Bluetooth module and the position sensor is placed in the central part of the mobile platform. The robot uses two dual RFID reader-antenna systems placed transversely. The ultrasonic distance sensor that detects obstacles is placed centrally at the front of the robot. A Li-Po battery pack was used as a power source for the electronic system. The schematic structure of the robot's components is presented in Fig. 3a.

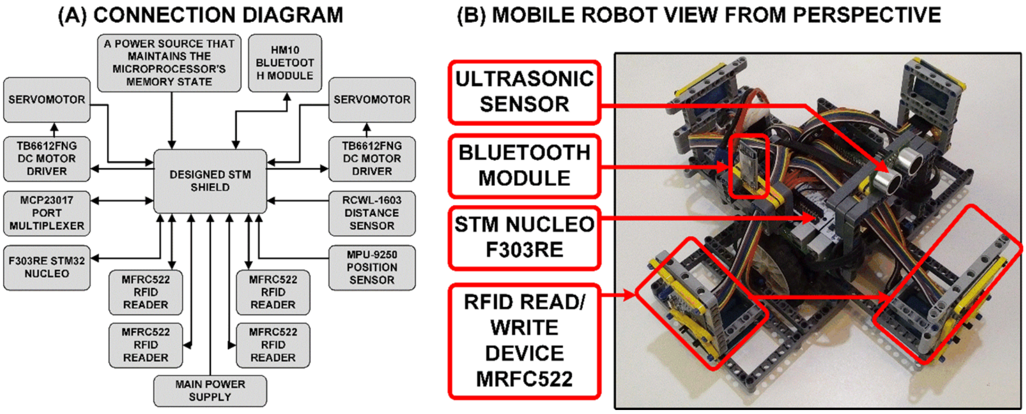

(a) (b)

Figure 3: (a) Simplified connection diagram of robot components, (b) view of the mobile robot from perspective

The mechanical structure of the robot is constructed with mechanical elements and drive units of the LEGO series. Each wheel is driven by an independent servo. Each has an internal reduction gear and has a maximum torque of 8 N/cm (maximum holding torque of 12 N/cm). The manufacturer declares their maximum speed at about 250 RPM, with a resolution accuracy of 360 pulses per revolution.

The robot prototype is presented in Fig. 3b. The robot skeleton consists of two independent and matched constructions: drive and electronic platform (including an ultrasonic distance sensor, Bluetooth module, and a set of RFID readers). It was decided to install the remaining electronic components, including engine control systems, 9DoF IMU sensor, and special RFID reader connector indirectly through a special extension board.

After analyzing the available solutions, it was decided to design and build a custom extension board called the STM Mindstorm Motors Shield. The design was made using the KiCad tool. Originally, the board was supposed to allow simultaneous control of several motors. During the work on the robot, extra elements were added to increase its functionality. As a result, a multifunctional module was created, extending the possibilities of the system by connecting additional peripherals with the use of dedicated connectors and communication interfaces, such as:

- two USART/UART buses on two different connectors,
- two I2C buses on two different connectors,
- three SPI buses on nine different connectors.

The module in the form of an extension board for the STM32 Nucleo-64 platform (in particular for the NUCLEO-F303RE) creates a coherent connection between the microprocessor and the rest of the peripheral systems used in the mobile robot (Fig. 4a). There are two battery connectors on the board, the main one and the second to maintain the microprocessor's memory in case of loss of the main power source. There is a Reverse Voltage Protection circuit (RVP), an Overvoltage Protection circuit (OVP), a voltage measurement circuit, an output for an external 5 V voltage stabilizer, and an unregulated linear voltage stabilizer with a 3.3 V Low-Droput (LDO). The board also features a MCP23017 port multiplexer and two TB6612FNG controllers, allowing for a total of four DC motors. A set of connectors for other peripherals is also placed on the expansion board. In addition, two additional connectors for the I2C and SPI buses were introduced, enabling further expansion of the mobile robot system in the future.

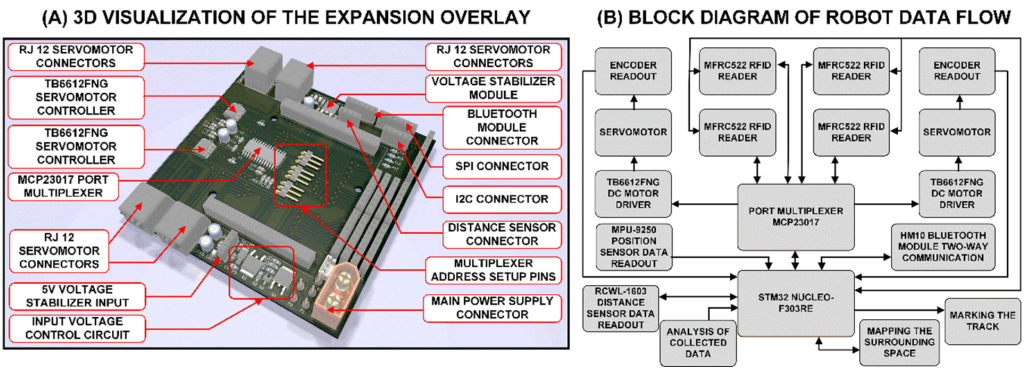

(a) (b)

Figure 4: (a) 3D visualization of the extension board, top view, (b) a simplified block diagram of data flow in the robot control program

The program controlling the operation of the mobile robot was written in the Arduino IDE (Integrated Development Environment). The software consists of many modules, which include functions controlling the voltage of the main power source, reading data from external sensors, encoders, and RFID readers, functions to analyze and process collected data, and communication with the master unit. Data processing in the program is quite complex; therefore, Fig. 4b shows a simplified block diagram of data flow between the most important program modules.

4. RFID grid arrangement

The use of a specific grid of RFID transponders makes it possible to build an intelligent environment that will be used to determine the coordinates of sensors and to record the parameters of the environment and the path of movement of objects, as well as the characteristics of dynamic changes of parameters in the environment. Thus, this approach enables the implementation of an autonomous mobile robot control system [46]. The grid of transponders, the structure of its arrangement and the correlation of the distance between the transponders and the interrogation zone of the RFID system in the communication space can take different forms and significantly affect the number of transponders simultaneously detected. The greater number of transponders in the interrogation zone requires a longer time to recognize them using the multiple identification algorithm. This time affects the parameters of the movement of the mobile robot, especially the speed of the movement. The temporary lack of a transponder identified in the interrogation zone means that the navigation system loses its position data and must use additional sensors or algorithms to approximate the motion path.

A robot equipped with an RFID reader can map an area using information and coordinates stored in transponders located on the grid, which may have different arrangements. Two basic patterns may be considered, i.e., a square mesh (Fig. 5a) and a triangular mesh (Fig. 5b). Assuming that the areas of activity of individual transponders have a circular shape (with radius R), which is in line with the theoretical premises of total surface coverage [47], the optimal solution is to locate the transponders at the vertices of an equilateral triangle (with side length: a). This type of mesh should provide smaller no-reading zones as shown in Figs. 5c and 5d [48, 52].

A MathCad application [49] was developed to simulate structures of transponders on a surface. Two types of mesh were analyzed: triangular and square grids. The transponder grid of transponders is based on a parallel structure, so it can be freely expanded. Regardless of the size of the surface, the area to be analyzed will always be limited. This is shown in Fig. 6.

For the comparison of both grid configurations, identical areas with dimensions of 0.45×0.45 m were adopted. The distances between the transponders in both types of grid (triangular D_T and square D_K) are closely related to each other. The most rational scenario is chosen, ensuring the presence of at least one transponder, regardless of the relative position of the reader's antenna to the transponders. The above assumption leads to the dependence:

$$D_T = \frac{3}{2} \cdot \sqrt{\frac{3}{2}} \cdot D_K . \tag{1}$$

Considering the above dependence (1), $D_T = 0.092$ m and $D_K = 0.05$ m were assumed. The trajectory of a mobile object on the grid can be freely defined.

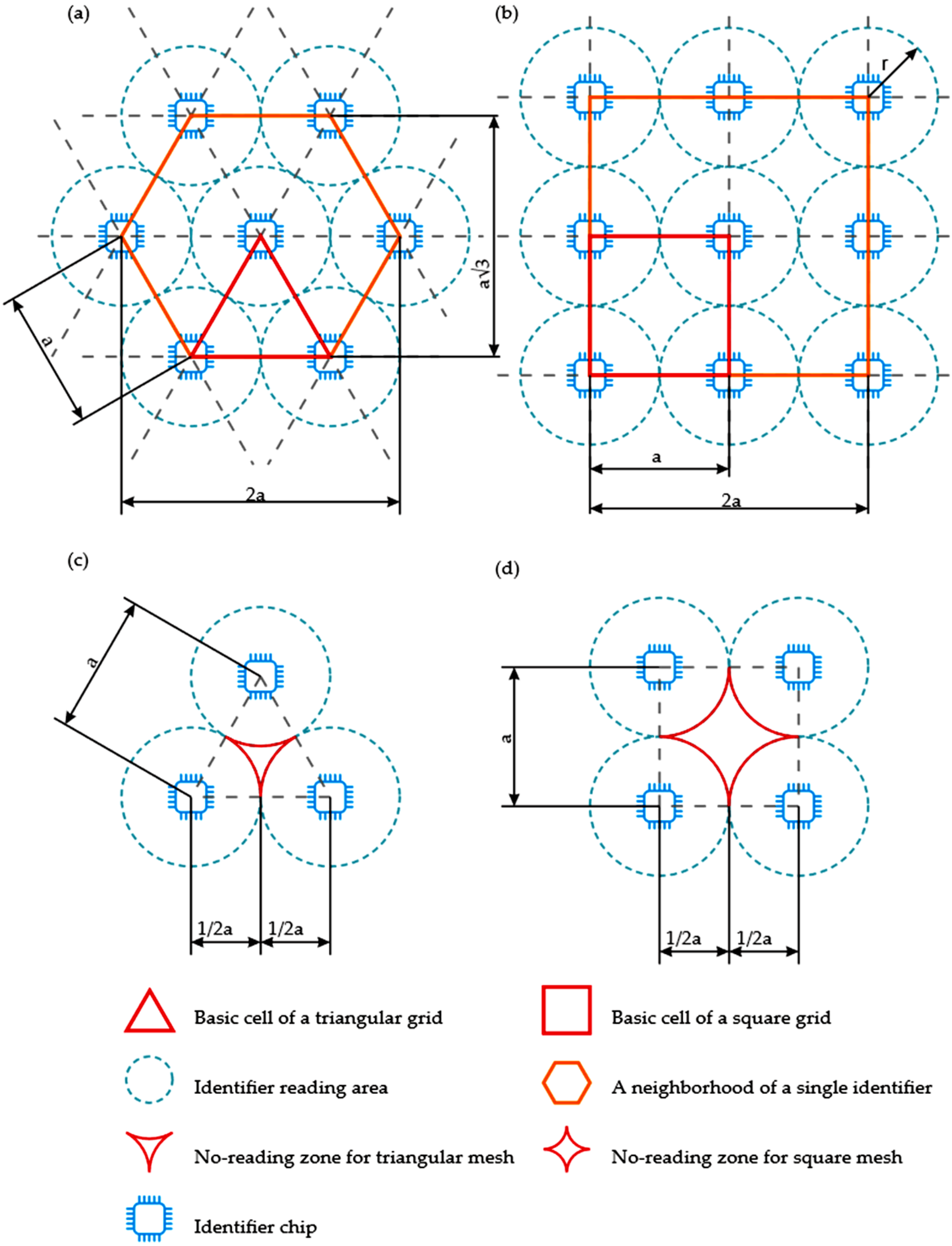

Figure 5: Basic RFID transponders: (a) triangular grid, (b) square grid, (c) no-read zone of the triangular grid, (d) no-read zone of the square grid

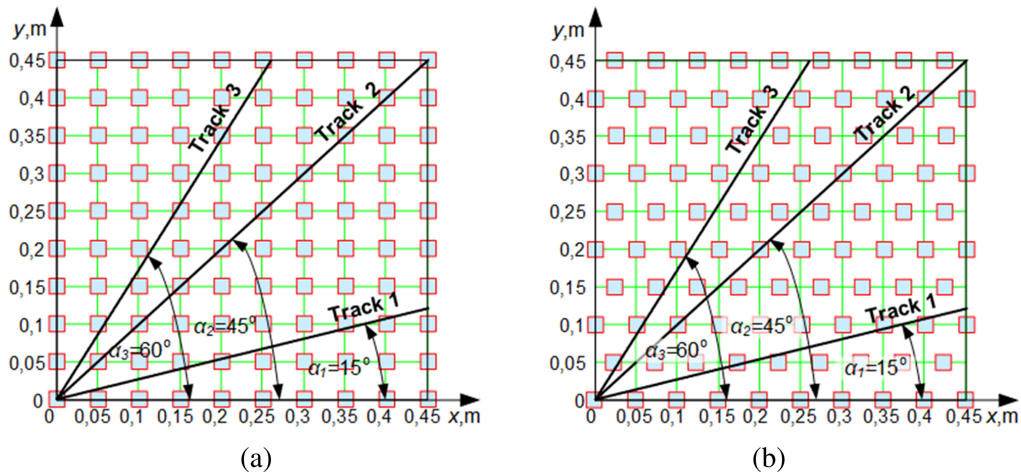

Figure 6: Assumptions for the simulation of grid arrangements: (a) square, (b) triangular

However, to simplify the calculations, the movement of the point along a straight line in three directions was assumed (Fig. 7). The shape of the interrogation zone was assumed to be a circle with a defined radius R. The x-axis was divided into 100 equidistant lines, and the steps of analyzing individual motion trajectories correspond to their projections on the x-axis for the subsequent discretization steps. It follows that the scope of the analysis of successive steps is limited to the shortest projection of the motion trajectory on the x-axis. It is the projection of Track 3 and determines the scope of the analysis in the range $\langle 0;\, 0.26\ \text{m}\rangle$.

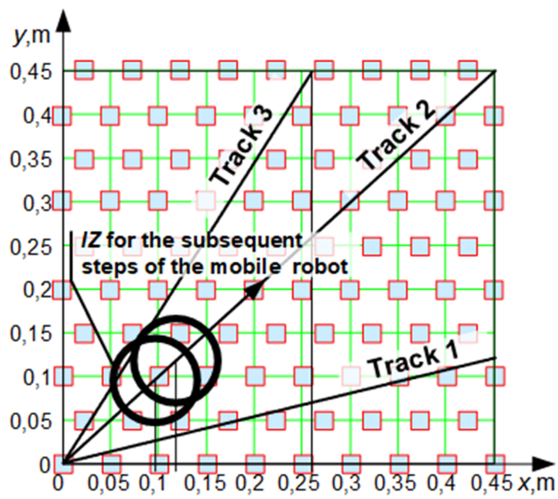

Figure 7: The interrogation zone and the limit of the considered simulation

The correlation of two grid arrangements with the size of the area of correct operation of the RFID system is presented below. The changing parameter is the radius R of the interrogation zone. In the individual graphs shown in Fig. 8, the number of transponders in the interrogation zone was compared for the square grid and the triangular grid, when changing the position of the RFID reader antenna according to the assumed trajectories of movement.

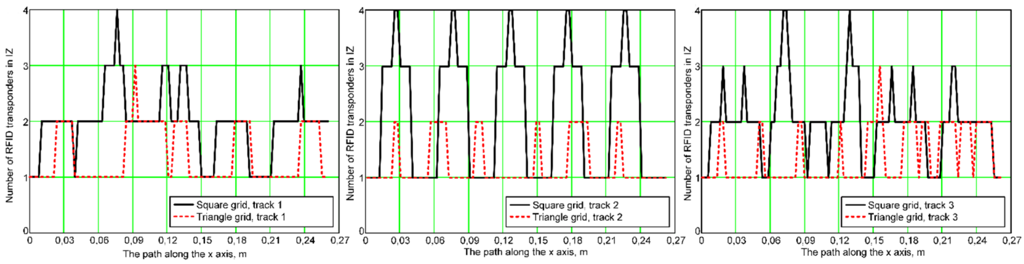

(a) (b) (c)

Figure 8: Number of transponders in the interrogation zone with radius R = 0.04 m

In the case considered in Fig. 8, the radius of the interrogation zone was chosen in such a way that at least one transponder is always present in this area, and the number of transponders for surface coverage is minimal under this condition. The radius of the interrogation zone for such assumptions is R = 0.04 m.

The arrangement of transponders has a significant impact on the number of transponders in the zone of correct operation, as well as the dynamics of changes in this number. For comparison purposes, statistical analysis was performed according to dependence.

$$Sr_{KwTr} = \frac{\sum_{k=1}^{100} \dfrac{l_{IdKw_k} - l_{IdKw_k}}{l_{IdKw_k}}}{100} \cdot 100\% = \sum_{k=1}^{100} \frac{l_{IdKw_k} - l_{IdKw_k}}{l_{IdKw_k}}\,, \% \tag{2}$$

where: k is the step of the mobile object along the x-axis, l_{IdKw_k} – the number of transponders in the interrogation zone of the RFID system for the square grid, l_{IdTr_k} – the number of transponders in the interrogation zone of the RFID system for the triangular grid.

In each case, the number of transponders is greater for the square grid by more than 20% on average. For example: for Track 1: $Sr_{KwTr} \approx 24\%$, for Track 2: $Sr_{KwTr} \approx 20\%$, and for Track 3: $Sr_{KwTr} \approx 21\%$.

Changing the size of the correct operation area (R = 0.15 m) so that a larger number of transponders (on average of a dozen or so) is identified at any position of the RFID reader antenna, gives the results shown in Fig. 9. As before, the number of transponders is greater for the square grid, by more than 30% on average (Track 1: $Sr_{KwTr} \approx 33\%$, Track 2: $Sr_{KwTr} \approx 35\%$, Track 3: $Sr_{KwTr} \approx 29\%$). In the first stage of the movement (up to about 0.12 m), a rapid increase in the number of transponders can be observed, which is caused by reaching the place where the interrogation zone is fully covered with the area marked with transponders.

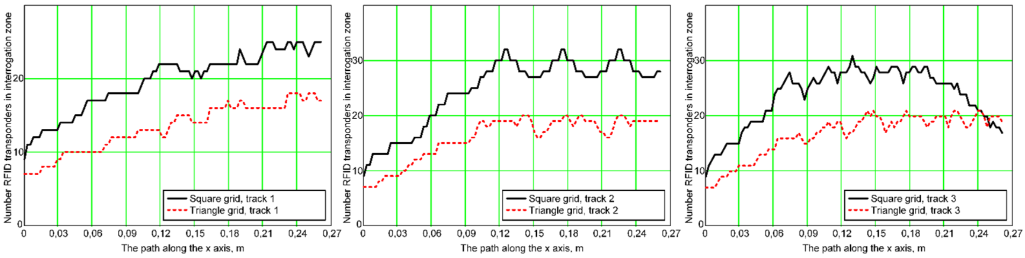

(a) (b) (c)

Figure 9: Number of transponders in the interrogation zone with radius $R = 0.15$ m

Based on the above results, it can be concluded that the use of the square grid allows us to increase the resolution of the navigation system compared to the triangular grid. In turn, this has a negative impact on information processing time. Control of possible traffic jam is more difficult, demand for computing power of the control system increases, and available speed of movement decreases.

5. Navigation and mapping algorithm

The arrangement of the RFID grid affects the way the robot moves from one transponder to another. In the square grid, each transponder has four closer neighbors and four further neighbors. If all eight transponders are considered adjacent, the motion trajectory can be changed to 45, 90, or 135 degrees. On the triangular grid, each transponder has six closest neighbors. The possible movement of the robot to the next transponder is possible without changing the trajectory or turning 60 or 120 degrees.

The algorithm for the operation of the navigation and mapping system follows the assumptions presented earlier. Figure 10 shows the overall workflow of robot navigation.

The algorithm uses the movement database, which stores information about the transponders and robot movements. When the system has no movement data in the database, the robot uses the information stored in the memory of each transponder and decides on further movement. The data in the database are then synchronized with the data read from the transponders. Thus, it is possible for

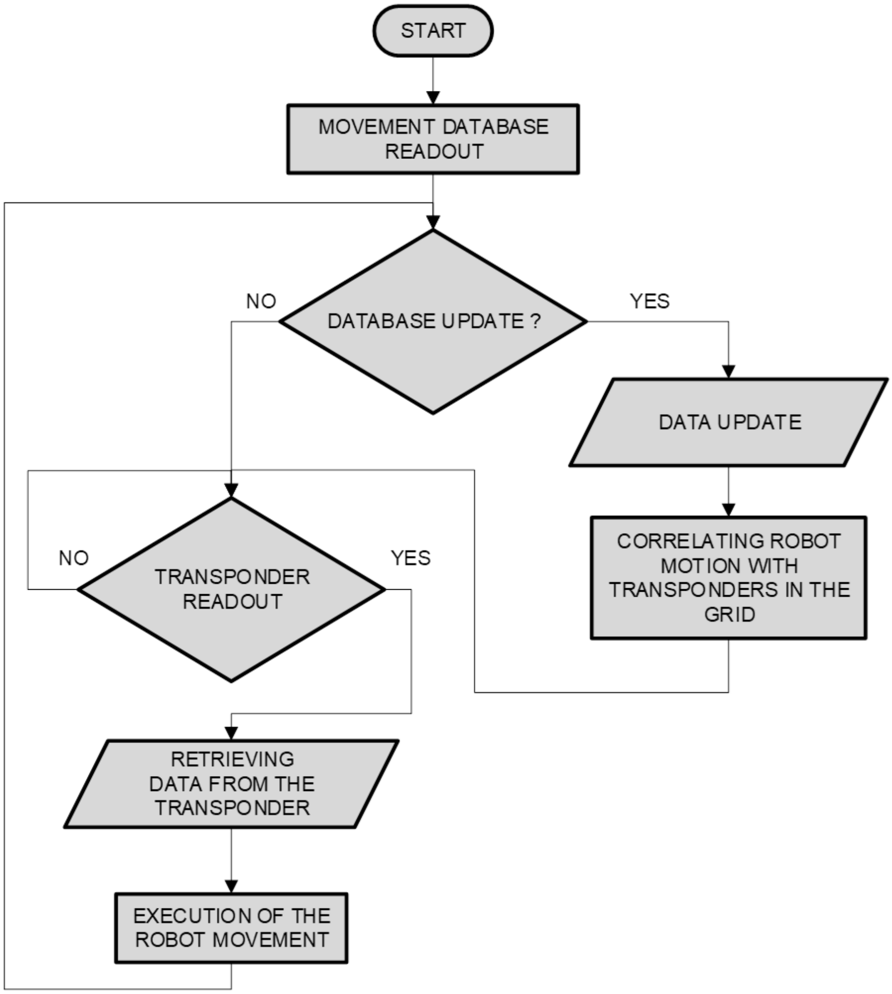

Figure 10: Robot Navigation and Mapping Algorithm

the robot to operate under conditions where there is no preloaded list of expected transponders and no list of pre-assigned actions.

Based on the unique identification number of the transponder and the movement action, the robot can perform a defined action. The prototype solution assumes that the default action is set to 0, which means that there is no movement. The other actions for the square grid are defined as follows: “Forward” is 1, “Rotate 90 degrees clockwise” is 2 and “Rotate 90 degrees counterclockwise” is 3, and so on. These actions are assigned to selected transponders and correspond to the specific type of grid. The algorithm that considers the actions defined in this way is presented in Fig. 11.

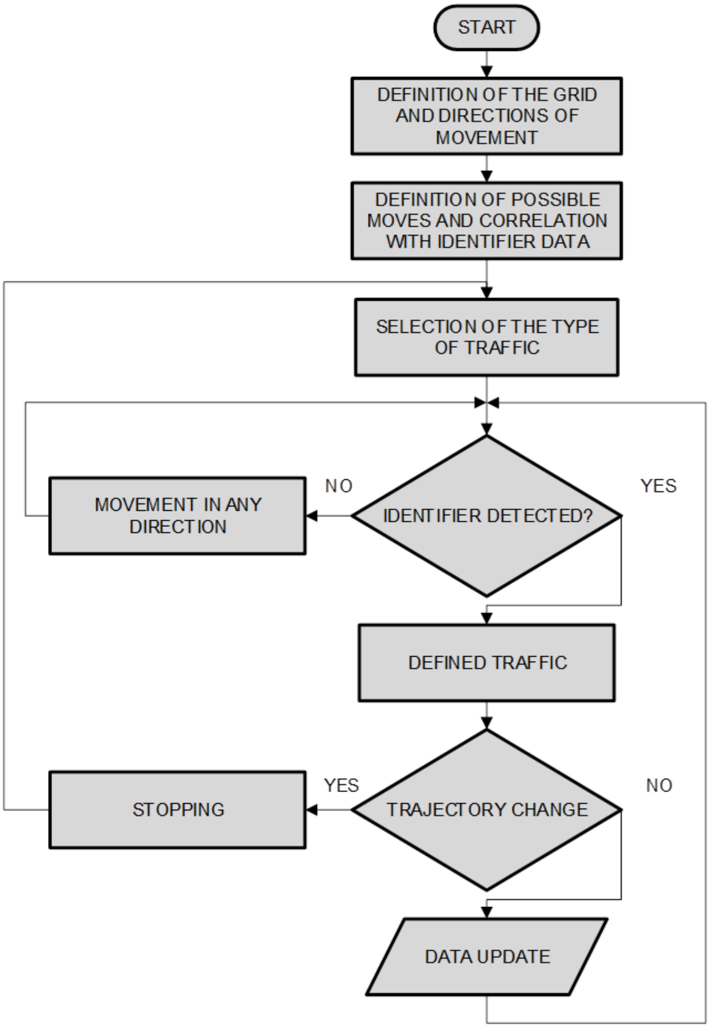

Figure 11: Algorithm for determining the movement trajectory

6. Determining the location of a moving object

One of the main tasks in the navigation of a mobile object is determining the current location. Here, this is done by reading data from transponders currently located in the interrogation zone. The arrangement of transponders on the surface over which the mobile object moves is of great importance here [50,51]. Section 5 presents a comparison of two arrangements (square, triangle) in terms of the number of transponders located in the zone of correct operation of the reader antenna so the accuracy of the location can be assessed.

Figure 12 shows two arrangements of transponders with marked routes of movement of the mobile object. In this case, a larger number of tracks (Track 0 . . . Track 17) is considered to increase the simulation precision. As before, the analyzed area has dimensions of 0.45 m $\times$ 0.45 m, and the distances between the transponders are selected so that there is at least one transponder in the interrogation zone, regardless of the location of the robot (Fig. 13).

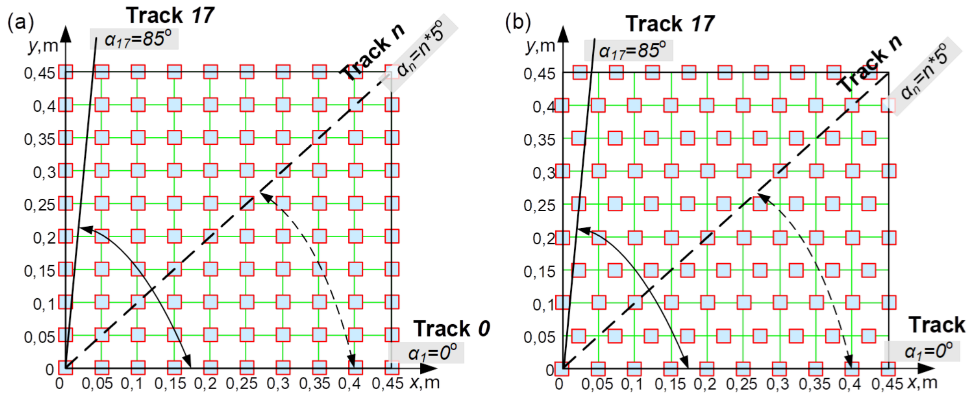

Figure 12: The robot paths

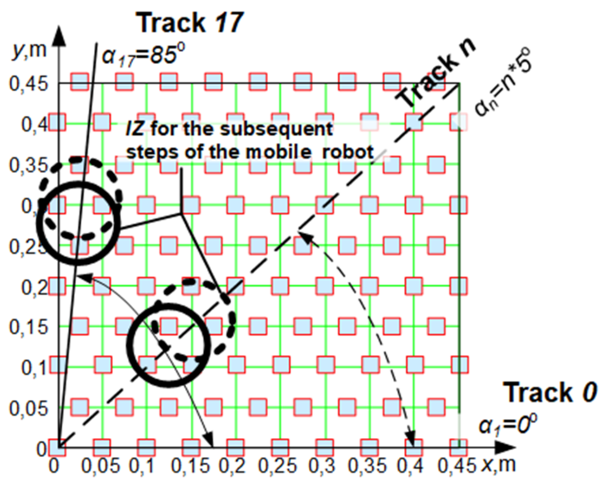

Figure 13: The interrogation zone and the limit of robot movement

The robot moved in a straight line. Analysis of many directions of movement (different angles of inclination in relation to the x axis) considered all possible directional components of any trajectory of its movement. Figure 14 shows the maximum distances, which, depending on the trajectory of movement and for different configurations of the placement of transponders, illustrate the minimum accuracy of the determined location of the object.

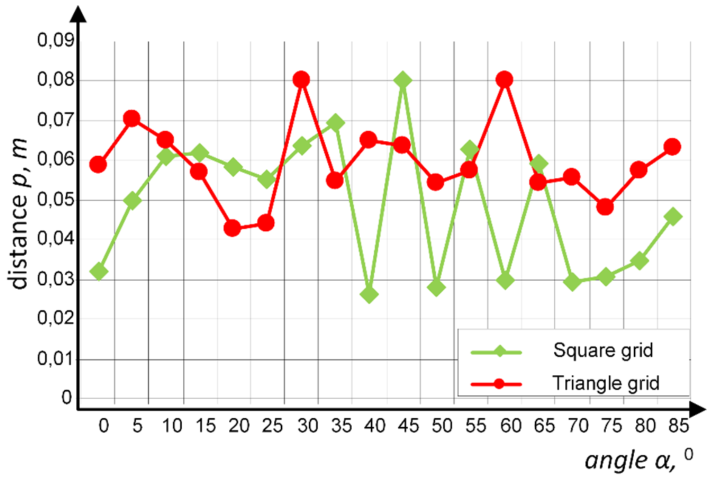

Figure 14: The greatest distance for a fixed number of transponders

In general, the inaccuracy error in determining the position of the robot depends on the direction of the robot's movement in relation to the surface, and in the worst case it is:

$$\sqrt{2} \cdot D_K \tag{3}$$

for the square grid, and:

$$\frac{2 \cdot \sqrt{3}}{3} \cdot D_T \tag{4}$$

for the triangular grid.

For both cases, it has the same maximum value, which results from the assumptions made when determining the transponder arrangement, and it may reach the value of 0.08 m in the analyzed case. It should be noted that the maximum error in determining the location is rarely achieved, on average remaining at a much lower value. On the other hand, when comparing the two arrangements in terms of location error, it should be stated that the square grid has higher location accuracy.

The use of a single antenna in the localization process, to determine the orientation of a mobile object, requires additional software procedures, including memorizing the previous position or additional movement of the object. Significantly improving this process involves the use of a second antenna, which additionally allows for a substantial increase in the efficiency of mobile object localization. It is recommended that the distance DA used for the square grid be as follows:

$$D_A = n \cdot \frac{\sqrt{2}}{2} \cdot D_K\,, \quad \text{where:} \quad n = 1, 3, 5, \ldots \tag{5}$$

and for the square grid:

$$D_A = n \cdot \frac{\sqrt{3}}{3} \cdot D_T\,, \quad \text{where:} \quad n = 1, 3, 5, \ldots \tag{6}$$

An example simulation of changes in the number of identifiers in the areas of correct operation of both antennas is shown in Fig. 15 for the square grid and Fig. 16 for the triangular grid.

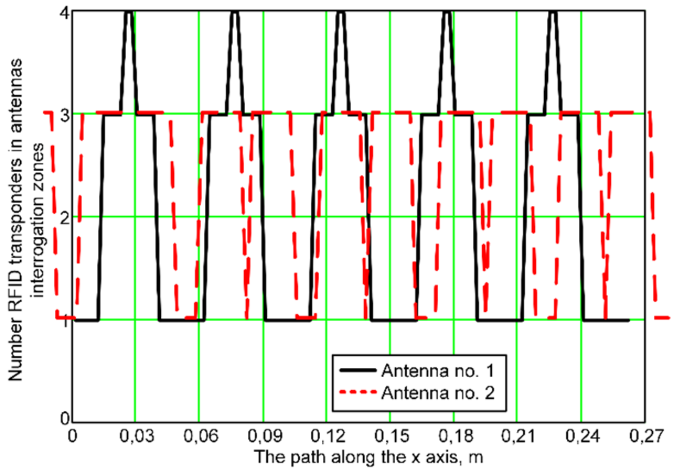

Figure 15: Number of transponders in the robot antennas interrogation zone for the square grid

Since the mobile robot prototype has been equipped with 2 dual reader-antenna systems, the analyses and simulations for a system with two antennas also apply here. The robot uses a single hardware bus to communicate with RFID readers. These RFID readers act as slaves, each activated through a dedicated line, incapable of initiating data transmission independently. In the case of two or more antennas, readers are controlled and activated in a specific software manner as described in [53]. Consequently, at any given moment, only one reader emits a carrier, thereby avoiding interference between antennas. The system may operate in polling and interrupt modes. Polling continuously monitors peripherals, consuming processor time and bus capacity. In RFID polling, the microcontroller regularly queries for transponder data. The interrupt mode generates a signal about events using a falling edge on the interrupt line.

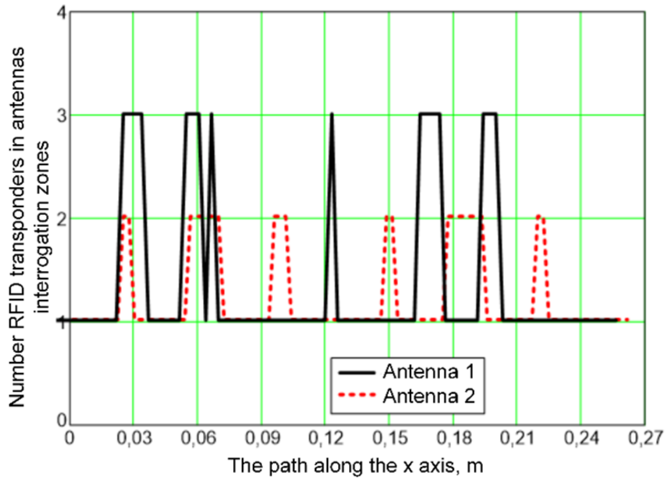

Figure 16: Number of transponders in the robot antennas interrogation zone for the triangle grid

7. Conclusion

The automatic navigation and mapping system presented in the article considers two types of the transponder grid. The triangular grid is more economical and requires fewer transponders. The rectangular grid, on the other hand, is characterized by greater possibilities in terms of location and freedom of movement. An additional improvement introduced in the presented robot prototype concerns the use of multiple RFID reader-antenna sets, thanks to which it is easier to determine the orientation on the surface.

References

[1] A. Motroni, F. Bernardini, A. Buffi, P. Nepa and B. Tellini: Self-locating RFID robot for tag localization in retails. IEEE International Conference on RFID, Atlanta, GA, USA, (2021). DOI: 10.1109/RFID52461.2021.9444384.

[2] M. Morenza-Cinos, V. Casamayor-Pujol and R. Pous: Stock visibility for retail using an RFID robot. *International Journal of Physical Distribution and Logistics Management*, **49**(10), (2019), 1020–1042. DOI: 10.1108/IJPDLM-03-2018-0151.

[3] W. Gueaieb and M.S. Miah: An intelligent mobile robot navigation technique using RFID technology. *IEEE Transactions on Instrumentation and Measurement*, **57**(9), (2008), 1908–1917. DOI: 10.1109/TIM.2008.919902.

[4] S. Lin and P. Wang: Design of a barcode identification system. IEEE International Conference on Consumer Electronics, Taiwan, (2014). DOI: 10.1109/ICCE-TW.2014.6904077.

[5] A. Eleni: Control of medical robotics and neurorobotic prosthetics by non-invasive brain-robot interfaces via EEG and RFID technology. 8th IEEE International Conference on BioInformatics and BioEngineering, Athens, Greece, (2008). DOI: 10.1109/BIBE.2008.4696838.

[6] K. Lakshmi Narayanan, Dr. N. Muthu Kumaran, G. Rajakumar, Hameedhul Arshadh, I. Dinesh and V. Caleb: Design and fabrication of medicine delivery robots for hospitals. (2019). International Conference on Recent Trends in Computing, Communication and Networking Technologies, Chennai, Tamilnadu, India, (2019). DOI: 10.2139/ssrn.3432156.

[7] T. Deyle, H. Nguyen, M. Reynolds and C. Kemp: RFID-guided robots for pervasive automation. *IEEE Pervasive Computing*, **9**(2), (2010), 37–45. DOI: 10.1109/MPRV.2010.17.

[8] E. DiGiampaolo and F. Martinelli: A robotic system for localization of passive UHF-RFID tagged objects on shelves. *IEEE Sensors Journal*, **18**(20), (2018), 8558–8568. DOI: 10.1109/JSEN.2018.2865339.

[9] H. Wu, B. Tao, Z. Gong, Z. Yin and H. Ding: A standalone RFID-based mobile robot navigation method using single passive tag. *IEEE Transactions on Automation Science and Engineering*, **18**(4), (2021), 1529–1537. DOI: 10.1109/TASE.2020.3008187.

[10] D. Monarca, P. Rossi, R. Alemanno, F. Cossio, P. Nepa, A. Motroni, R. Gabbrielli, M. Pirozzi, C. Console and M. Cecchini: Autonomous vehicles management in agriculture with Bluetooth low energy (BLE) and passive Radio Frequency Identification (RFID) for obstacle avoidance. *Sustainability*, **14** (2022). DOI: 10.3390/su14159393.

[11] Y. He, D. Wang, F. Huang, Y. Zhang, R. Zhang and X. Yan: A RFID-integrated framework for tag anti-collision in UAV-aided VANETs. *Remote Sensing*, **13** (2021). DOI: 10.3390/rs13224500.

[12] O. Nakamatsu and T. Wada: A study on RFID-based arbitrary point-to-point navigation and path recovery system for mobile robots. 31st International Telecommunication Networks and Applications Conference, Sydney, Australia, (2021). DOI: 10.1109/ITNAC53136.2021.9652150.

[13] E. DiGiampaolo and F. Martinelli: Range and bearing estimation of an UHF-RFID tag using the phase of the backscattered signal. *IEEE Journal of Radio Frequency Identification*, **4**(4), (2020), 332–342. DOI: 10.1109/JRFID.2020.3016168.

[14] S. Han, H. Lim and J. Lee: An efficient localization scheme for a differential-driving mobile robot based on RFID system. *IEEE Transactions on Industrial Electronics*, **54**(6), (2007), 3362–3369. DOI: 10.1109/TIE.2007.906134.

[15] E. DiGiampaolo and F. Martinelli: A passive UHF-RFID system for the localization of an indoor autonomous vehicle. *IEEE Transactions on Industrial Electronics*, **59**(10), (2012), 3961–3970. DOI: 10.1109/TIE.2011.2173091.

[16] A. Papapostolou and H. Chaouchi: RFID-assisted indoor localization and the impact of interference on its performance. *Journal of Network and Computer Applications*, **34**(3), (2011), 902–913. DOI: 10.1016/j.jnca.2010.04.009.

[17] P. Jankowski-Mihułowicz and M. Węglarski: Determination of 3-dimentional interrogation zone in anticollision RFID systems with inductive coupling by using Monte Carlo method. *Acta Physica Polonica A*, **21**(4), (2012), 936–940. DOI: 10.12693/APhysPolA.121.936.

[18] M. Konieczny, B. Pawłowicz, J. Potencki and M. Skoczylas: Application of RFID technology in navigation of mobile robot. 21st European Microelectronics and Packaging Conference (EMPC) and Exhibition, Warsaw, Poland, (2017). DOI: 10.23919/EMPC.2017.8346907.

[19] G. Mylonopoulos, A.R. Chatzistefanou, A. Filotheou, A. Tzitzis, S. Siachalou and A.G. Dimitriou: Localization, tracking and following a moving target by an RFID equipped robot. IEEE International Conference on RFID Technology and Applications, Delhi, India, (2021). DOI: 10.1109/RFID-TA53372.2021.9617436.

[20] A. Isrofi, B. Setiawan and S. Wibowo: Automated guided vehicle (AGV) navigation control using matrix method applying Radio Frequency Identification (RFID) point address. International Conference on Electrical and Information Technology, Malang, Indonesia, (2021). DOI: 10.1109/IEIT53149.2021.9587440.

[21] S.P. Subramanian, J. Sommer, S. Schmitt and W. Rosenstiel: RIL – reliable RFID based indoor localization for pedestrians. 16th International Conference on Software, Telecommunications and Computer Networks, Split, Croatia, (2008). DOI: 10.1109/SOFTCOM.2008.4669483.

[22] Y. Chia-Yu and H. Wei-Chun: An indoor positioning system based on the dual-channel passive RFID technology. *IEEE Sensors Journal*, **18**(11), (2018), 4654–4663. DOI: 10.1109/JSEN.2018.2828044.

[23] M.M. Soltani, A. Motamedi and A. Hammad: Enhancing cluster-based RFID tag localization using artificial neural networks and virtual reference

tags. International Conference on Indoor Positioning and Indoor Navigation, Montbeliard, France, (2013). DOI: 10.1109/IPIN.2013.6817886.

[24] C.-W. Park, G.-Y. Choi, J.-S. Chae and B.-G. Kim: A design for passive RFID system on a chip. 11th International Conference on Advanced Communication Technology, Gangwon, Korea (South), (2009).

[25] A. Tzitzis, S. Megalou, S. Siachalou, T.G. Emmanouil, A. Filotheou, T.V. Yioultsis and A.G. Dimitriou: Trajectory planning of a moving robot empowers 3D localization of RFID tags with a single antenna. *IEEE Journal of Radio Frequency Identification*, **4**(4), (2020), 283–299. DOI: 10.1109/JRFID.2020.3000332.

[26] P. Jankowski-Mihułowicz and M. Węglarski: Factors affecting the synthesis of autonomous sensors with RFID interface. *Sensors*, **19**(20), (2019). DOI: 10.3390/s19204392.

[27] E. Abad, B. Mazzolai, A. Juarros, D. Gómez, A. Mondini, I. Sayhan, A. Krenkow and T. Becker: Fabrication process for a flexible tag microlab. Proceedings of SPIE, 6589 (2007).

[28] A. Oprea, J. Courbat, N. Bârsan, D. Briand, N.F. de Rooij and U. Weimar: Temperature, humidity and gas sensors integrated on plastic foil for low power applications. *Sensors and Actuators B: Chemical*, **140** (2009), 227–232. DOI: 10.1016/j.snb.2009.04.019.

[29] P. Jankowski-Mihułowicz and M. Węglarski: Definition, characteristics and determining parameters of antennas in terms of synthesizing the interrogation zone in RFID systems. In P.C. Crepaldi and T.C. Pimenta (Eds.), Radio Frequency Identification, Intech, London, UK, 2017, Chapter 5, 65–119.

[30] K. Finkenzeller: *RFID Handbook – Fundamentals and Applications in Contactless Smart Cards, Radio Frequency Identification and Near-Field Communication*. 3rd ed. Chichester, Wiley, 2010.

[31] P. Jankowski-Mihułowicz, B. Pawłowicz and G. Pitera: Zagadnienie wymiany danych w systemie RFID pasma HF z autonomicznym identyfikatorem półpasywnym. *Przegląd Elektrotechniczny*, **91** (2015), 74–77, (in Polish).

[32] P. Jankowski-Mihułowicz, M. Węglarski and W. Lichoń: A procedure for validating impedance parameters of HF/UHF RFID transponder antennas. In R. Hanus, D. Mazur, C. Kreischer (Eds.), Methods and Techniques of Signal Processing in Physical Measurements. MSM2018. Lecture Notes in Electrical Engineering, 548, 101–118, Springer, Cham, 2019. DOI: 10.1007/978-3-030-11187-8_9.

[33] P. Jankowski-Mihułowicz, G. Tomaszewski and M. Węglarski: Flexible antenna design for HF RFID semi-passive transponder in ink-jet technology. *Przegląd Elektrotechniczny*, **4** (2015), 1–5. DOI: 10.15199/48.2015.04.01.

[34] D.M. Dobkin: *The RF in RFID: UHF RFID in Practice*. 2nd ed. Oxford, Newnes, 2012.

[35] C. Balanis: *Antenna Theory*. 4th ed. Hoboken, Wiley. 2016.

[36] I. Pratt and S. Zhong: A heuristically designed high-frequency RFID antenna head for use within libraries. IEEE International Conference on RFID Technology and Applications, Pisa, Italy, (2019). DOI: 10.1109/RFID-TA.2019.8892112.

[37] F. Pebay-Peyroula and J. Reverdy: A true full-duplex communication between HF contactless reader and card. IEEE International Conference on RFID-Technologies and Applications, Sitges, Spain, (2011). DOI: 10.1109/RFID-TA.2011.6068681.

[38] M. Wobak, M. Gebhart and U. Muehlmann: Physical limits of batteryless HF RFID transponders defined by system properties. IEEE International Conference on RFID-Technologies and Applications, Nice, France, (2012). DOI: 10.1109/RFID-TA.2012.6404500.

[39] S. Rizkalla, R. Prestros and C.F. Mecklenbräuker: Characterizing chip's behavior of HF RFID cards during load modulation. IEEE International Conference on RFID Technology and Application, Warsaw, Poland, (2017). DOI: 10.1109/RFID-TA.2017.8098638.

[40] J. Grosinger, B.J.B. Deutschmann, L. Zöscher, M. Gadringer and F. Amtmann: HF RFID tag chip impedance measurements. *IEEE Transactions on Instrumentation and Measurement*, **71** (2022), 1–11. DOI: 10.1109/TIM.2021.3130664.

[41] M. Benamara, M. Grzeskowiak, M. Salhi, G. Lissorgues, A. Diet and Y. Le Bihan: Array subloops reader antenna for HF RFID tracking. IEEE International Conference on RFID Technology and Application, Warsaw, Poland, (2017). DOI: 10.1109/RFID-TA.2017.8098892.

[42] International Organization for Standardization/International Electrotechnical Commission. Identification Cards – Contactless Integrated Circuit Cards – Proximity Cards. ISO/IEC, Geneva, Switzerland, 2016, p. 14443-4.

[43] International Organization for Standardization/International Electrotechnical Commission. Identification Cards – Contactless Integrated Circuit Cards – Vicinity Cards. ISO/IEC, Geneva, Switzerland, 2006, p. 15693.

[44] R.R.A. Syms, O. Sydoruk and M.C.K. Wiltshire: Magneto-inductive HF RFID system. *IEEE Journal of Radio Frequency Identification*, **5**(2), (2021), 148–153. DOI: 10.1109/JRFID.2020.3042719.

[45] X. Liang, C. Zhang, J. Hu, T. Zhou and J. Ouyang: Design of a new HF RFID reader antenna. International Conference on Microwave and Millimeter Wave Technology, Nanjing, China, (2021). DOI: 10.1109/ICMMT52847.2021.9617864.

[46] M. Hubacz, B. Pawlowicz and B. Trybus: Exploring a surface using RFID grid and group of mobile robots. In R. Szewczyk, C. Zieliński and M. Kaliczyńska (Eds.), Advances in Intelligent Systems and Computing, 743, Automation 2018 Advances in Automation, Robotics and Measurement Techniques, Springer, (2018), 490–499.

[47] R. Kershner: The number of circles covering a set. *American Journal of Mathematics*, **61**(3), (1939), 665–671.

[48] W. Kalita and M. Skoczylas: Application of RFID technique for object location on plane area. 33st International IMAPS-CPMT Poland Conference, Gliwice-Pszczyna, Poland, (2009).

[49] P. Jankowski-Mihułowicz, W. Kalita, M. Skoczylas and M. Węglarski: Wpływ struktury przestrzennego rozmieszczenia identyfikatorów-czujników RFID na jakość procesu sterowania autonomicznych obiektów. *Elektronika – Konstrukcje, Technologie, Zastosowania*, 6 (2010), 154–157, (in Polish).

[50] W. Kalita and M. Skoczylas: System nawigacji autonomicznych obiektów mobilnych z wykorzystaniem techniki RFID. *Elektronika – Konstrukcje, Technologie, Zastosowania*, **8** (2010), 81-85.

[51] M. Szumowski, M. Żórawska and T. Zielińska: Preview control applied for humanoid robot motion generation. *Archives of Control Sciences*, **29**(1), (2019), 111–132. DOI: 10.24425/acs.2019.127526.

[52] E. Jezierski, P. Łuczak, P. Smyczyński and D. Zarychta: Human-robot cooperation in sorting of randomly distributed objects. *Archives of Control Sciences*, **29**(4), (2019), 603–615. DOI: 10.24425/acs.2019.131228.

[53] M. Hubacz, B. Pawłowicz and B. Trybus: Using multiple RFID readers in mobile robots for surface exploration. In R. Szewczyk, C. Zieliński and M. Kaliczyńska (Eds.), Automation 2019. Advances in Intelligent Systems and Computing, 920 Springer, Cham. DOI: 10.1007/978-3-030-13273-6_42.